Method Development of Damage Detection in Asymmetric Buildings

Yi Wang*, David P Thambiratnam, Tommy HT Chan, and Andy Nguyen

School of Civil Engineering and Built Environment, Queensland University of Technology (QUT), Brisbane, Australia

ABSTRACT

Aesthetics and functionality requirements have caused most buildings to be asymmetric in recent times. Such buildings exhibit complex vibration characteristics under dynamic loads as there is coupling between the lateral and torsional components of vibration, and are referred to as torsionally coupled buildings. These buildings require three dimensional modelling and analysis. In spite of much recent research and some successful applications of vibration based damage detection methods to civil structures in recent years, the applications to asymmetric buildings has been a challenging task for structural engineers. There has been relatively little research on detecting and locating damage specific to torsionally coupled asymmetric buildings. This paper aims to compare the difference in vibration behaviour between symmetric and asymmetric buildings and then use the vibration characteristics for predicting damage in them. The need for developing a special method to detect damage in asymmetric buildings thus becomes evident. Towards this end, this paper modifies the traditional modal strain energy based damage index by decomposing the mode shapes into their lateral and vertical components and to form component specific damage indices. The improved approach is then developed by combining the modified strain energy based damage indices with the modal flexibility method which was modified to suit three dimensional structures to form a new damage indicator. The procedure is illustrated through numerical studies conducted on three dimensional five-story symmetric and asymmetric frame structures with the same layout, after validating the modelling techniques through experimental testing of a laboratory scale asymmetric building model. Vibration parameters obtained from finite element analysis of the intact and damaged building models are then applied into the proposed algorithms for detecting and locating the single and multiple damages in these buildings. The results obtained from a number of different damage scenarios confirm the feasibility of the proposed vibration based damage detection method for three dimensional asymmetric buildings.

KEYWORDS: Vibration based damage detection, asymmetric building, modal flexibility, modal strain energy, structural damage, finite element method

1 Introduction

An asymmetric building can be defined as one in which there is either geometric, stiffness or mass eccentricity. In such buildings, the lateral and torsional components of the response are coupled leading to complex behaviour. The dynamic behaviour of an asymmetric building can result in interruption of force flow, stress concentration and torsion [1]. This torsion can lead to an increase in shear force, lateral deflection and ultimately cause failure. The development and application of a robust technique to detect and locate damage at its onset is thus important in order to avoid the possible catastrophic structural failure. Traditionally, damage in civil structures were often assessed by visual inspection or Non-Destructive Testing (NDT) techniques such as X-ray and ultrasonic waves to measure cracks and permanent deformations [2], all of which require the damaged region to be accessible. The drawbacks of these methods are that the damaged region might not be readily accessible and the collected data might not be adequate for effective prediction of the remaining life of a structure. This has led to the development of vibration based methods which are global in nature and which consider the

*Corresponding author.
E-mail address: y90.wang@hdr.qut.edu.au (Y. Wang)

changes in the vibration characteristics of the structure [3]. Vibration Based Damage Identification (VBDI) methods have effectively addressed the drawback of traditional methods. Many VBDI methods basically rely on measuring the vibration properties such as natural frequencies and mode shapes of both the healthy (or base line) and damaged structures. The collected data is analysed which can then be used solely or along with the vibration data from a numerical model of the structure to detect and locate damages. Initially, implementation and operation of VBDI techniques have been mainly in aircraft structures, railway systems and machinery [4]. During the past decades, structural engineers have made great efforts to identify damage in civil structures. Most of the existing studies based on vibration based methods for identifying damage used numerical simulations or non-in-situ experimental techniques. Generally, the performance of a damage indicator or a damage identification technique depends on the type of structures [5]. Structures that received greatest research interest include beams [6, 7], plate elements [8, 9], trusses [10-12], steel frames [13, 14], offshore platforms [15-17] and bridges [5, 18, 19]. Despite the many successful applications in those structures in recent years, the identification of damage in complex structures such as 3D buildings, especially asymmetric buildings, remains a challenging task for structural engineers. There is relatively less investigation on detecting and locating damage in torsionally coupled asymmetric buildings.

Using natural frequency change as the basic feature for damage detection was one of the most common approaches. Frequencies can be easily measured with a small number of sensors and they are robust again measurement noise [20]. However, frequencies have been shown to be sensitive to temperature while their changes are unable to provide spatial information and hence damage detection methods relying solely on change in natural frequency may not be sufficient for locating damage [21, 22]. The advantage of using mode shapes compared with natural frequencies is that mode shapes contain spatial information and are less sensitive to environmental effects. Although mode shape based methods contain spatial information, it is hard to capture accurate and reliable mode shapes in large structures with a limited number of sensors, especially if higher modes are deemed more favourable than the lower modes for damage detection [23]. Methods based on modal flexibility have also received considerable attention from many researchers. The motivation of using this method is that the complete vibration parameters for damage detection are not required [24]. The literatures confirm that the Modal Flexibility (MF) based method has a wide variety of applications in damage detection studies. However there is no application in detecting and locating damage in large scale asymmetric building structures. Modal Strain Energy (MSE) based method was first developed by Stubbs and Kim [25], [26]. It has been successfully applied to data from a damaged bridge and has been found to be the most accurate algorithm in comparison with several other algorithms that are being currently investigated [17]. The principle of this method is that damage reduces structure stiffness and hence changes the strain energy. This method has been used in further studies by Law, Shi and Zhang [12] to detect and locate damage in structures with incomplete and noisy measured modal data. Their method was validated by using the results from laboratory experiments on a two storey steel frame structure. The experimental program was divided into three stages: (1) expanding of the measured mode shapes, (2) locating damage using elemental strain energy difference, and (3) quantifying damage based on sensitivity of natural frequency. Results showed that the proposed method was capable of detecting and quantifying single or multiple damages in the experimental structure. Au, Cheng, Tham and Bai [27] further extended the method developed by Law, Shi and Zhang [12] by adopting a micro-genetic algorithm in the damage quantification stage. Shi, Law and Zhang [28], [29] proposed a technique for locating damage using the MSE Change Ratio (MSECR) of each structural element. This method only requires mode shapes and the elemental stiffness matrix. The application of the proposed method to a truss structure and a two-storey frame structure demonstrated its capability to locate single and multiple damages. Shih, Thambiratnam and Chan [19] proposed a multi-criteria approach incorporating MF and MSE based methods for detecting damages in slab-on-girder bridges. It was found that for single damage both flexibility and strain energy changes provided accurate results for locating damage. However for

multiple damage cases, only the MSE based method was capable of accurately locating the damage.

From the review of the many approaches above, it is evident that the MF change and MSE change methods have the capability to detect and locate damage. Moreover, the overall review of the literature indicated that it is unrealistic to expect damage to be reliably detected in all cases by using a single damage index especially in multiple damage scenarios. Combined methods have provided a better chance of structural damage detection. The focus of the present study is to develop a multi-criteria approach (MCA) based on a modified version of the traditional MSE method, along with the MF method. The method will be validated by simulated data of two structures (i) 5 storey symmetric structure and (ii) 5 storey asymmetric structure which are modelled and analysed utilizing ANSYS software [30].

2 Comparative study of symmetric and asymmetric building

2.1 Structural Models

A 3 dimensional five-storey symmetric frame structure [17] is considered and simulated using Finite Element software ANSYS as presented in Figure 1(a). The lengths of the members are presented in Figure 1. Young's modulus is equal to 2.1×10^{11} Pa for all members, and the cross section area for all members is $A=2.825\times10^{-3}$ m^2.

The asymmetric frame structure is designed by doubling the density of beam elements (30, 31, 38, and 39) as show in Figure 1(b). All the other properties are same as in the symmetric model. These two simple forms of buildings are chosen to show that even in such simpler forms, the asymmetric nature of building model (b) has challenges and emphasises the need for a specific method for damage detection in asymmetric buildings.

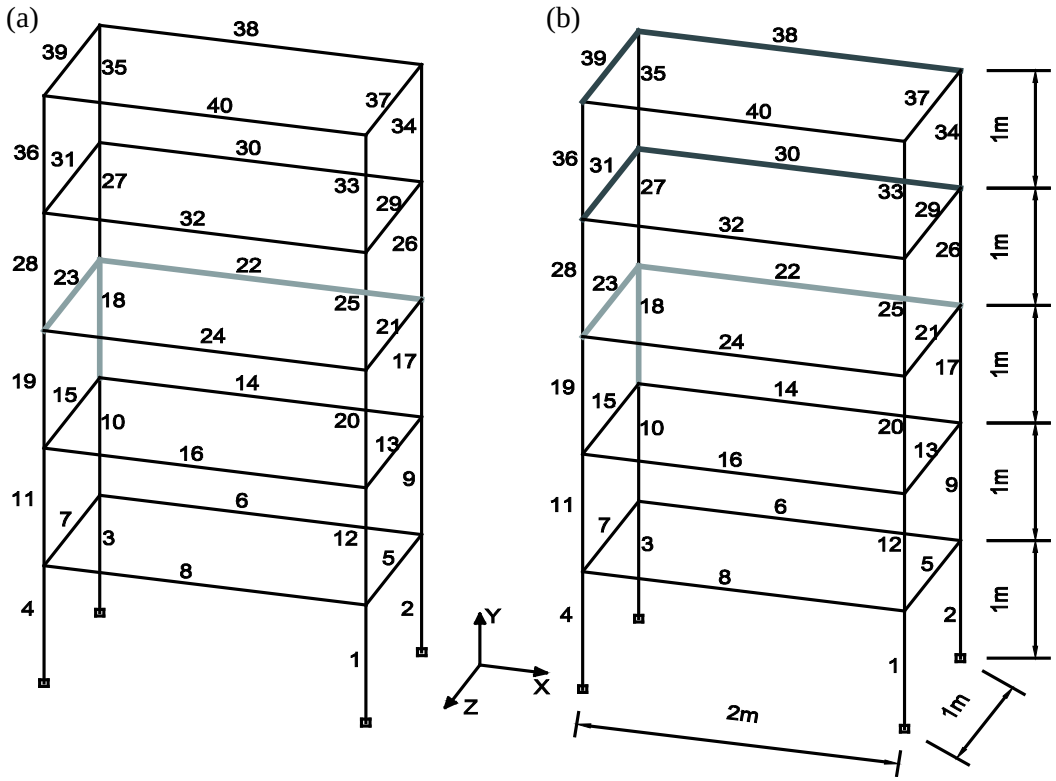

Fig. 1. 3D Structural diagrams of two building models (a) symmetric building model and (b) asymmetric building model

It has been observed that the first two mode shapes are significantly different for the symmetric and asymmetric structures. Comparison of the first 2 mode shapes of the symmetric and asymmetrical framed structures is shown in Figure 2. For the symmetric building, the first

mode vibrates along to the longer side of the cross-section and the second mode is in the direction of the shorter side. It is realized that the first mode vibrates in the 'weaker' direction of the structure. In the current numerical example, the weak side is in the direction of the longer side; when all cross sections and material properties remain identical for all beams, the stiffness of the beams are inversely proportional to their lengths. For the asymmetric building, it is clear that the first mode vibrates dominantly in the direction of the longer side, but the joint displacements are considerably decreased compared to the symmetric building as this lateral vibration is coupled with torsional vibration in clockwise direction due to the mass eccentricity. The second mode vibrates dominantly in the direction of the shorter side; and as with the first mode, the amplitudes of the joint displacement also decrease due to the coupling with the torsional mode in the anti-clockwise sense. These differences in the vibration characteristics between the two models, especially the presence of the coupled vibration modes in the asymmetric structure create the complexity in using the vibration data for damage detection in asymmetric structures.

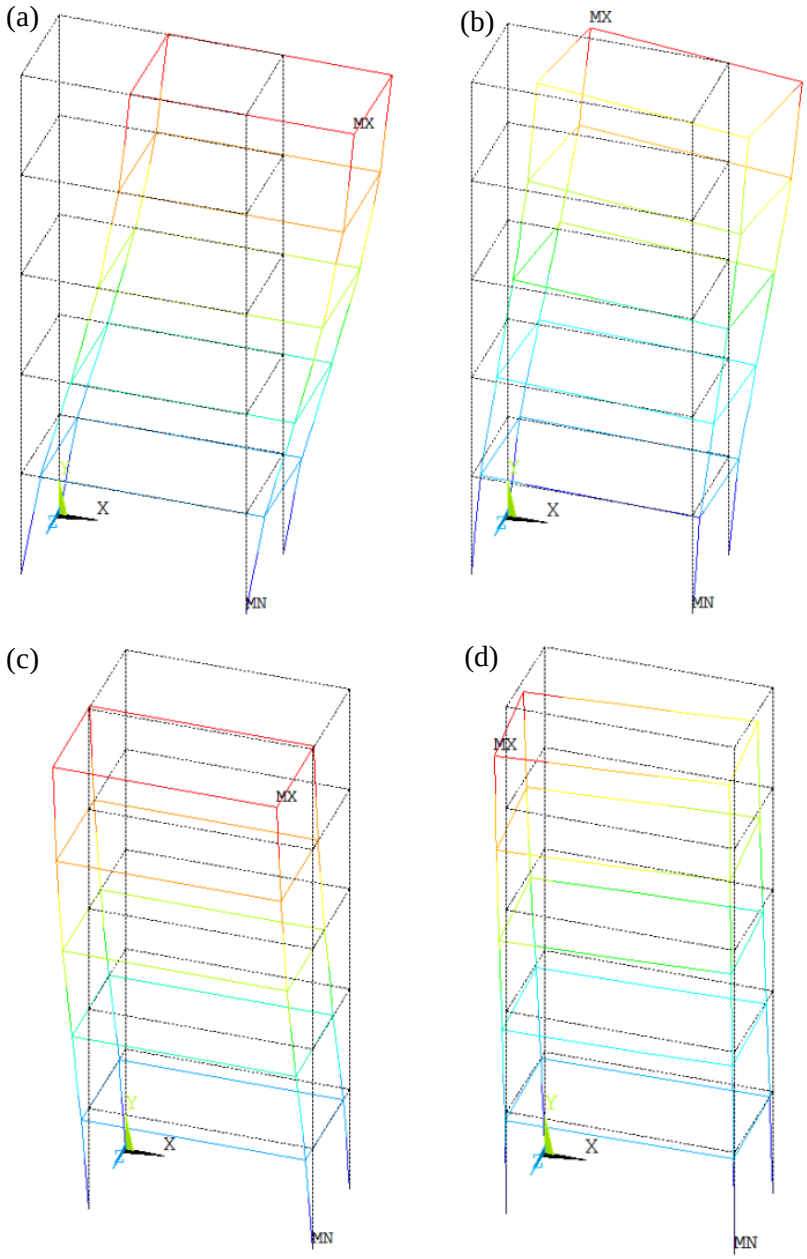

Fig. 2. Typical mode shapes of the two models (a) first mode of symmetric model (b) first mode of asymmetric model (c) second mode of symmetric model and (d) second mode of asymmetric model

2.2 Traditional method

In order to compare the difference between symmetric and asymmetric buildings in damage detection, the earlier modal strain energy based methods which proposed by Stubbs, Kim and Farrar [26] is used in this study. For a linear, intact structure with N_e elements, the i^{th} modal strain energy of a structure is given by

$$\mathbf{U}_i = \mathbf{\Phi}_i^{\mathrm{T}} \mathbf{K} \mathbf{\Phi}_i$$

where **K** is the system stiffness matrix which assembles all element stiffness matrices, and $\mathbf{\Phi}_i$ is the i^{th} intact mode shape. Modal strain energy U_{ij} of the j^{th} element is defined as

$$U_{ij} = \mathbf{\Phi}_i^{\mathrm{T}} \mathbf{K}_j \mathbf{\Phi}_i$$

where $\mathbf{K}_j$ is the element stiffness matrix. For the i^{th} mode, the fraction of MSE in the j^{th} member is given by

$$f_{ij} = \frac{U_{ij}}{\mathbf{U}_i}$$

The damage in a member is simulated in this study by effectively reducing the Young's modulus in material, and hence $\mathbf{K}_j$ could be written as

$$\mathbf{K}_j = E_j \mathbf{K}_{j0}$$

where E_j is a parameter representing the Young's modulus of j^{th} element, and the matrix $\mathbf{K}_{j0}$ contains only geometric quantities. Similarly, for a damaged structure we have

$$\mathbf{U}_i^d = \mathbf{\Phi}_i^{d\mathrm{T}} \mathbf{K}^d \mathbf{\Phi}_i^d, \; U_{ij}^d = \mathbf{\Phi}_i^{d\mathrm{T}} \mathbf{K}_j^d \mathbf{\Phi}_i^d \qquad (5), (6)$$

$$f_{ij}^d = \frac{U_{ij}^d}{\mathbf{U}_i^d}, \; \mathbf{K}_j^d = E_j^d \mathbf{K}_{j0} \qquad (7), (8)$$

Stubbs and Kim [25] state that when number of element N_e is large, both f_{ij} and f_{ij}^d tend to be much less than unity. This will give

$$\frac{\left(f_{ij}^d + 1\right)}{\left(f_{ij} + 1\right)} = 1$$

Substituting Eqs. (3) and (7) into Eq. (9) yields

$$\frac{(\, U_{ij}^d + \, \mathbf{U}_i^d)\mathbf{U}_i}{(U_{ij} + \mathbf{U}_i)1 \; \mathbf{U}_i^d} = 1$$

Substituting Eqs. (1), (2), (5) and (6) into Eq. (10) and rearranging we obtain

$$\frac{E_j^d}{E_j} \frac{\left[\mathbf{\Phi}_i^{d\mathrm{T}} \mathbf{K}_{j0} \mathbf{\Phi}_i^d + \left(\frac{1}{E_j^d}\right) \mathbf{\Phi}_i^{d\mathrm{T}} \mathbf{K}^d \mathbf{\Phi}_i^d\right] \mathbf{U}_i}{\left[\mathbf{\Phi}_i^{\mathrm{T}} \mathbf{K}_{j0} \mathbf{\Phi}_i + \left(\frac{1}{E_j}\right) \mathbf{\Phi}_i^{\mathrm{T}} \mathbf{K} \mathbf{\Phi}_i\right] \mathbf{U}_i^d} = 1$$

The indicator β_{ij} to detect damage can be defined to be the ratio of intact material strength and damaged material strength E_j/E_j^d and imposing the approximations $\mathbf{K} \approx E_j\mathbf{K}_0$ and $\mathbf{K}^d \approx E_j^d\mathbf{K}_0$, we obtains

$$\beta_{ij} = \frac{E_j}{E_j^d} = \frac{(\mathbf{\Phi}_i^{d\mathrm{T}}\mathbf{K}_{j0}\mathbf{\Phi}_i^d + \mathbf{\Phi}_i^{d\mathrm{T}}\mathbf{K}_0\mathbf{\Phi}_i^d)\mathbf{\Phi}_i^{\mathrm{T}}\mathbf{K}\mathbf{\Phi}_i}{(\mathbf{\Phi}_i^{\mathrm{T}}\mathbf{K}_{j0}\mathbf{\Phi}_i + \mathbf{\Phi}_i^{\mathrm{T}}\mathbf{K}_0\mathbf{\Phi}_i)\mathbf{\Phi}_i^{d\mathrm{T}}\mathbf{K}\mathbf{\Phi}_i^d}$$

If *Nm* modes are considered in the damage detection process, the following formation can be used

$$\beta_j = \frac{E_j}{E_j^d} = \frac{\sum_{i=1}^{Nm}\{(\mathbf{\Phi}_i^{d\mathrm{T}}\mathbf{K}_{j0}\mathbf{\Phi}_i^d + \mathbf{\Phi}_i^{d\mathrm{T}}\mathbf{K}_0\mathbf{\Phi}_i^d)\mathbf{\Phi}_i^{\mathrm{T}}\mathbf{K}\mathbf{\Phi}_i\}}{\sum_{i=1}^{Nm}\{(\mathbf{\Phi}_i^{\mathrm{T}}\mathbf{K}_{j0}\mathbf{\Phi}_i + \mathbf{\Phi}_i^{\mathrm{T}}\mathbf{K}_0\mathbf{\Phi}_i)\mathbf{\Phi}_i^{d\mathrm{T}}\mathbf{K}\mathbf{\Phi}_i^d\}}$$

For a more robust damage detection criterion, the normalized indicator is given by

$$MSE_j = \frac{\beta_j - \bar{\beta}}{\sigma_\beta}$$

where $\mathbf{K}_j$ is the element stiffness matrix of j^{th} element, $\mathbf{K}_{j0}$ contains only geometric quantities and $\mathbf{K}$ is the system stiffness matrix which assembles all element stiffness matrices. $\mathbf{\Phi}_i$ is the i^{th} intact mode shape and $\mathbf{\Phi}_i^d$ is the i^{th} damaged mode shape.

2.3 Results and discussions

The following damage scenarios are considered to further investigate the effects of torsional coupling in damage detection of the two different structures. Three single-damage cases have been proposed

Table 1
Damage cases studied

Case Number	Damaged Element Type	Element Number	Damage Percent (%)
Case 1	long span beam	22	5%
Case 2	short span beam	23	5%
Case 3	vertical column	18	5%

2.3.1 Damage Case 1

The first scenario is damage in long span beam element 22 with 5% loss of Young's modulus. Figure 3(a) shows the results for the symmetric model. In the first mode, the response component is dominant in x-direction (Figure 2). It is hence reasonable to have a larger value of the damage index in the column elements 17, 18, 26, and 27, as their nodal coordinates are shared in this structure. Therefore, damage is not only expected to be detected in the damaged member itself, but also in the members connected to it. And as the first mode predominantly vibrates in the long side direction, all long-span beams are (with negligible deformation) moving along with the columns; however, all short-span beams exhibit noticeable elongation and contraction especially those at upper floors to hold together the two planar frames formed by the longer-span beams and columns. In this case it is expected that the long-span beam damage could be more influenced by the second mode which vibrates in z-direction (short-span direction), and this has been proved by the results using the second mode.

Figure 3(b) presents the results for the asymmetric model. As seen from the first mode, due to torsional coupling the damage in the beam element 22 has a tendency to propagate to the beam elements 29 and 31 through the column elements that connect them. It is clearer to see this trend from the second mode. Due to torsional coupling, the damage in the longer-span beam 22 has been propagated to all beam elements of the model and the severity has a tendency to increase from lower level to upper level.

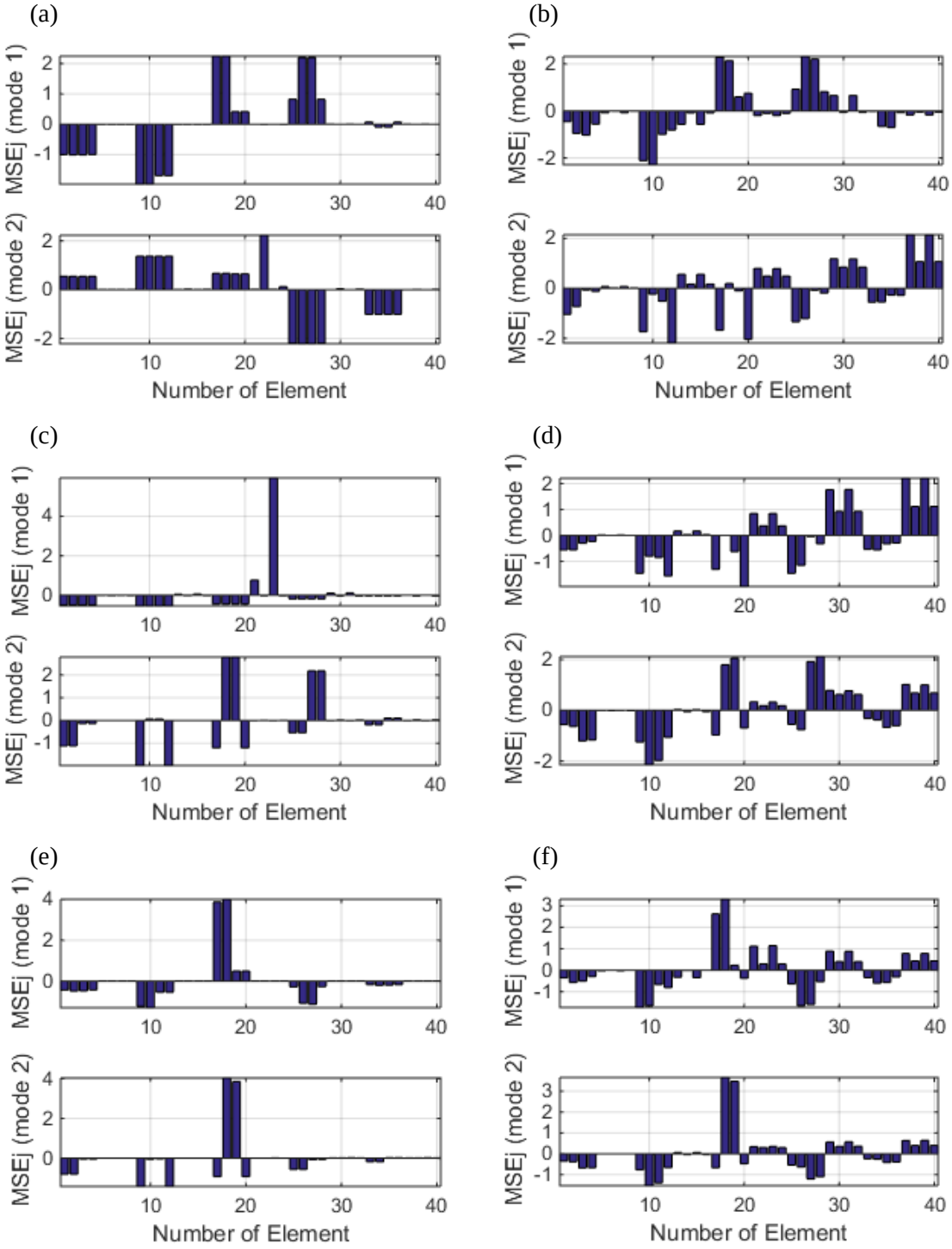

Fig. 3. Results of the symmetric and asymmetric models using Stubbs' damage index (a) symmetric model (case 1) (b) asymmetric model (case 1) (c) symmetric model (case 2) (d) asymmetric model (case 2) (e) symmetric model (case 3) and (f) asymmetric model (case 3)

2.3.2 Damage Case 2

The second scenario is damage in a short-span beam element 23 with 5% loss of Young's modulus. The results are presented in Figure 3(c) & (d). This damage has been successfully identified by the first mode of the symmetric model which vibrates in the x-direction. It confirms with the previous discussion that a mode vibrating predominantly in the z-direction must be utilized in the calculation for locating a damaged long-span beam. Similarly the results of asymmetric model also confirms well with the above discussion of the first damage scenario.

2.3.3 Damage Case 3

In this case as shown in Figure 3(e), the vibration of the first mode in the symmetric model is mainly in the x-direction. In view of the relative position between elements 17 and 18, it is reasonable that element 17 vibrates at a magnitude comparable to that of element 18. Therefore, when damaged element 18 shows a large value in the plot of the MSE based damage index, it is logical to have a large value on element 17 as well. In many ways, the results using the second mode display similar features as those with the first mode. As the direction of the vibration is now mainly in the z-direction, large values (of the damage index) are evident at elements 18 and 19, in contrast to those in elements 17 and 18 for the first mode.

The results of asymmetric model are present in Figure 3(f). Similarly to the damage case 1, damage of the column element has been propagated to all beam elements of the model due to the torsional coupling.

3 Modified method

From the results presented in the above section, it is evident that in asymmetric buildings, due to torsional coupling, the damage in a beam element has a tendency to influence the other beam elements connected to it and complicates the damage detection process. This tendency is different to what occurs in symmetric buildings in which damage in a beam does not influence the other beams in the vicinity and the damage can be detected more easily. Such a feature is also evident with columns in an asymmetric building. Probably due to their complex behaviour, considerably less work is reported in the literature on detecting and locating damage specific to torsionally coupled asymmetric buildings. It is therefore timely to address the problem of detecting and locating damage in such common but rather complicated building structures.

Structural members of an asymmetric frame structure predominantly have two types of elements (1) horizontal members (beams) and (2) vertical members (columns). Normally vibration modes of a building structure are mainly horizontal instead of vertical; in this case MSE change in the vertical members would be dominated by the lateral MSE. On the other hand, MSE change of the horizontal members would be contributed significantly by the vertical MSE [17]. Therefore in this study two damage indicators, a lateral damage indicator and a vertical damage indicator, are formulated by decomposing Stubbs' damage index. The modified damage indicator could be rewritten as

$$\beta_j^L = \frac{\sum_{i=1}^{Nm}\left\{\left(\boldsymbol{\Phi}_i^{Ld\mathrm{T}}\mathbf{K}_{j0}\boldsymbol{\Phi}_i^{Ld} + \boldsymbol{\Phi}_i^{Ld\mathrm{T}}\mathbf{K}_0\boldsymbol{\Phi}_i^{Ld}\right)\boldsymbol{\Phi}_i^{L\mathrm{T}}\mathbf{K}\boldsymbol{\Phi}_i^{L}\right\}}{\sum_{i=1}^{Nm}\left\{\left(\boldsymbol{\Phi}_i^{LT}\mathbf{K}_{j0}\boldsymbol{\Phi}_i^{L} + \boldsymbol{\Phi}_i^{LT}\mathbf{K}_0\boldsymbol{\Phi}_i^{L}\right)\boldsymbol{\Phi}_i^{Ld\mathrm{T}}\mathbf{K}\boldsymbol{\Phi}_i^{Ld}\right\}}$$

$$\beta_j^V = \frac{\sum_{i=1}^{Nm}\{(\boldsymbol{\Phi}_i^{Vd\mathrm{T}}\mathbf{K}_{j0}\boldsymbol{\Phi}_i^{Vd} + \boldsymbol{\Phi}_i^{Vd\mathrm{T}}\mathbf{K}_0\boldsymbol{\Phi}_i^{Vd})\boldsymbol{\Phi}_i^{V\mathrm{T}}\mathbf{K}\boldsymbol{\Phi}_i^{V}\}}{\sum_{i=1}^{Nm}\left\{\left(\boldsymbol{\Phi}_i^{V\mathrm{T}}\mathbf{K}_{j0}\boldsymbol{\Phi}_i^{V} + \boldsymbol{\Phi}_i^{V\mathrm{T}}\mathbf{K}_0\boldsymbol{\Phi}_i^{V}\right)\boldsymbol{\Phi}_i^{Vd\mathrm{T}}\mathbf{K}\boldsymbol{\Phi}_i^{Vd}\right\}}$$

Then the modified normalized indicator is defined as

$$MMSE_j^L = \frac{\beta_j^L - \overline{\beta^L}}{\sigma_{\beta^L}}$$

$$MMSE_j^V = \frac{\beta_j^V - \overline{\beta^V}}{\sigma_{\beta^V}}$$

where $\boldsymbol{\Phi}_i^L$ is the i^{th} intact mode shape using only the lateral components and $\boldsymbol{\Phi}_i^V$ is the i^{th} intact mode shape utilizing only the vertical components.

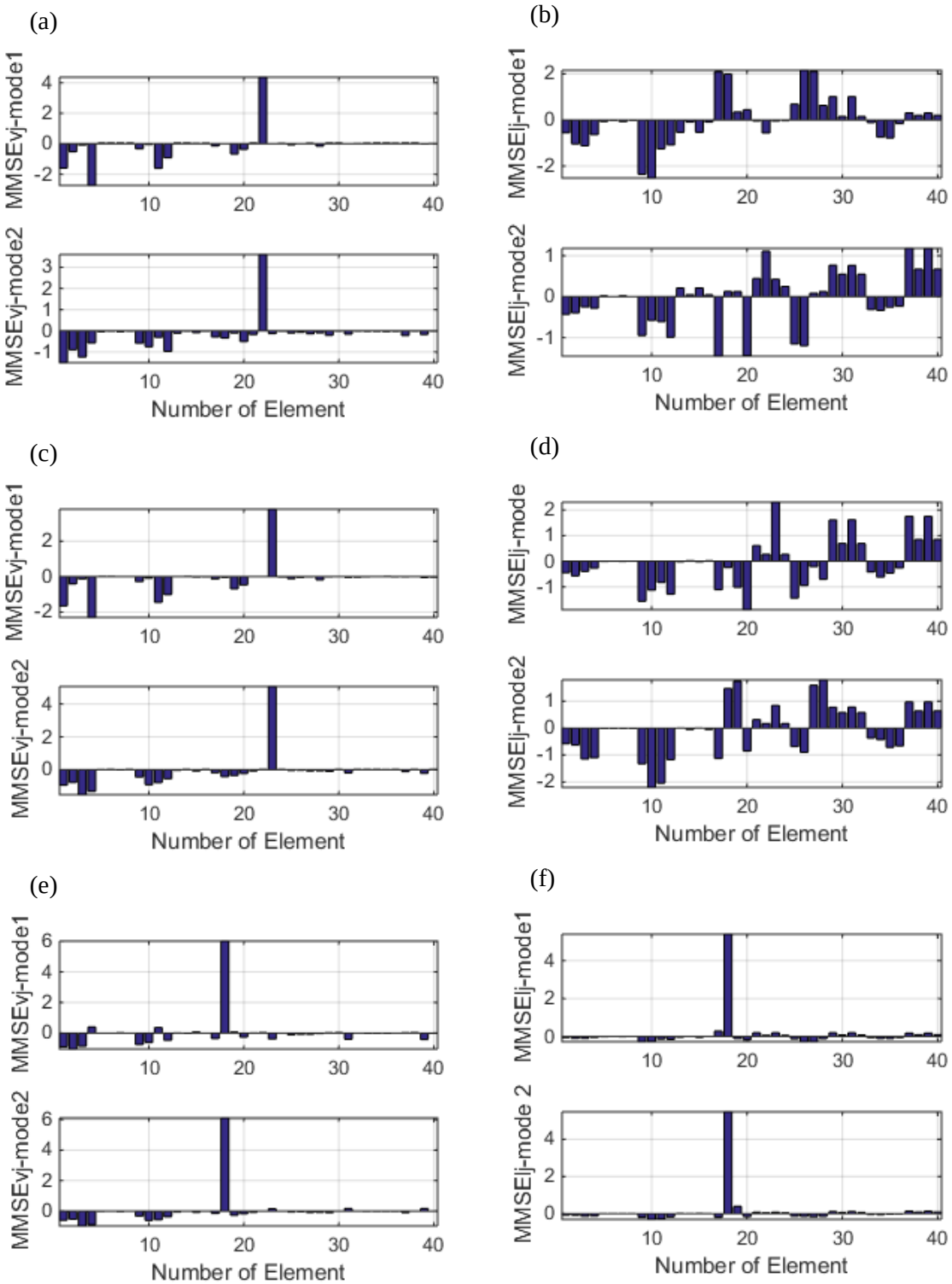

Fig. 4. Damage detection results using the modified method (a) vertical damage indicator (case 1) (b) lateral damage indicator (case 1) (c) vertical damage indicator (case 2) (d) lateral damage indicator (case 2) (e) vertical damage indicator (case3) and (f) lateral damage indicator (case 3)

The proposed modified method is illustrated through a numerical study. The results of damage case 1 are presented in Figure 4(a) and 4(b). It clearly demonstrates that the purposed vertical damage indicator has the capability to locate damage in the horizontal beam elements. The results of damage case 2 which are shown in Figure 4(c) and 4(d) confirm this capability. On the other hand, the lateral indicator shows good capability at locating damage in the vertical column element as shown in Figure 4(f). These findings confirm that proposed modified damage detection method is capable of locating damage in this asymmetric building structure.

However in real situations, there is no previous information on the location of damage, and since there are two indicators, it is difficult to establish whether the damage is in a beam or column, especially if there are multiple damages. In this case the modified modal flexibility (MMF) method could assist the proposed MMSE method to confirm the damaged member(s). $\mathbf{MMF}\%$, $\mathbf{MMSE}^{\mathrm{L}}$ and $\mathbf{MMSE}^{\mathrm{V}}$ could then be used together in the improved damage detection strategy as they will complement and supplement each other.

4 Improved method

Modal flexibility, $\mathbf{F}_h$ of an intact linear (one dimensional) structure can be obtained as [31]

$$\mathbf{F}_h = \left[\sum_{i=1}^{n} \frac{1}{\boldsymbol{\omega}_i^2} \boldsymbol{\Phi}_i \boldsymbol{\Phi}_i^{\mathrm{T}}\right]_h$$

where i and n are the mode number and total number of modes considered respectively, $\boldsymbol{\Phi}_i$ is the i^{th} mode shape, $\frac{1}{\boldsymbol{\omega}^2}$ is the reciprocal of the square of natural frequencies. In the above summation and all subsequent summations, it is implied that the terms with the repeated subscript (i) are summed over all the values of that subscript.

Evaluation of changes in the flexibility matrix of a structure was first proposed by Pandey and Biswas [24] as

$$\mathbf{MFC} = \mathbf{F}_d - \mathbf{F}_h = \left[\sum_{i=1}^{n} \frac{1}{\boldsymbol{\omega}_i^2} \boldsymbol{\Phi}_i \boldsymbol{\Phi}_i^{\mathrm{T}}\right]_d - \left[\sum_{i=1}^{n} \frac{1}{\boldsymbol{\omega}_i^2} \boldsymbol{\Phi}_i \boldsymbol{\Phi}_i^{\mathrm{T}}\right]_h$$

where $\mathbf{F}_h$ and $\mathbf{F}_d$ are MF matrices of the healthy and damaged structure respectively. The maximum absolute value in each column of the MF matrix corresponding to a specific node in the structure is then extracted and written as

$$\overline{\delta_j} = max_j|\delta_{kj}|$$

where δ_{kj} is element of $\mathbf{MFC}$. $\overline{\delta_j}$ is set as an indicator to measure the change of flexibility for each measurement location.

Wickramasinghe, Thambiratnam, Chan and Nguyen [32] improved this method for detecting damage in suspension bridges by normalizing the $\mathbf{MFC}$ by $\mathbf{F}_h$ as

$$\mathbf{MFC}\% = \frac{\mathbf{MFC}}{\mathbf{F}^h} \times 100\% = \frac{\left[\sum_{i=1}^{n} \frac{1}{\boldsymbol{\omega}_i^2} \boldsymbol{\Phi}_i \boldsymbol{\Phi}_i^{\mathrm{T}}\right]_d - \left[\sum_{i=1}^{n} \frac{1}{\boldsymbol{\omega}_i^2} \boldsymbol{\Phi}_i \boldsymbol{\Phi}_i^{\mathrm{T}}\right]_h}{\left[\sum_{i=1}^{n} \frac{1}{\boldsymbol{\omega}_i^2} \boldsymbol{\Phi}_i \boldsymbol{\Phi}_i^{\mathrm{T}}\right]_h}$$

For a three dimensional asymmetric building each node in a member of the structure contains 3 translational degrees of freedom (DOFs). In order to apply MF based method to asymmetric buildings the MF matrix $\mathbf{MFC}(2L + V)$ of j measurement locations will then be $3j \times 3j$ array instead of $j \times j$. Where L and V denote the lateral and vertical component of the mode shapes respectively. The modified $\mathbf{MMF}\%$ can then be expressed as

$$\mathbf{MMF}\% = \begin{bmatrix} \delta\%_{11} & \delta\%_{12} & \delta\%_{13} & \cdots & \delta\%_{1(3j-2)} & \delta\%_{1(3j-1)} & \delta\%_{1(3j)} \\ \delta\%_{21} & \delta\%_{22} & \delta\%_{23} & \cdots & \delta\%_{2(3j-2)} & \delta\%_{2(3j-1)} & \delta\%_{2(3j)} \\ \delta\%_{31} & \delta\%_{32} & \delta\%_{33} & \cdots & \delta\%_{3(3j-2)} & \delta\%_{3(3j-1)} & \delta\%_{3(3j)} \\ \vdots & \vdots & \vdots & \ddots & \vdots & \vdots & \vdots \\ \delta\%_{(k-2)1} & \delta\%_{(k-2)2} & \delta\%_{(k-2)3} & \cdots & \delta\%_{(k-2)(j-2)} & \delta\%_{(k-2)(3j-1)} & \delta\%_{(k-2)(3j)} \\ \delta\%_{(k-1)1} & \delta\%_{(k-1)2} & \delta\%_{(k-1)3} & \cdots & \delta\%_{(k-1)(j-2)} & \delta\%_{(k-1)(3j-1)} & \delta\%_{(k-1)(3j)} \\ \delta\%_{k1} & \delta\%_{k2} & \delta\%_{k3} & \cdots & \delta\%_{k(j-2)} & \delta\%_{k(3j-1)} & \delta\%_{k(3j)} \end{bmatrix}_{3j\times 3j} \quad (23)$$

We first consider the maximum absolute value from each column to form a single array (row) of **MMF**% as shown below

$$max_j\left|\delta\%_{kj}\right| = [max|\delta\%_{k1}|\ max|\delta\%_{k2}|\ max|\delta\%_{k3}| \cdot\cdot \cdot max\left|\delta\%_{k(3j-2)}\right|\ max\left|\delta\%_{k(3j-1)}\right|\ max\left|\delta\%_{k(3j)}\right|]_{1\times 3j}$$

Considering this (horizontal array), in sets of 3 values, we take the maximum absolute value $\delta\%_j$ from each set in the form

$$MMF\%(2L+V)_j = max(max_{(3j-2)}\left|\delta\%_{k(3j-2)}\right| : max_{(3j)}\left|\delta\%_{k(3j)}\right|)$$

As now there are three indicator, which may lead to confusion in the results, a new damage index (DI) is developed which combines the results of **MMF** and $\mathbf{MMSE}^L$ and the results of **MMF** and $\mathbf{MMSE}^V$ to obtain more accurate results. Due to torsional coupling, there will be some elements showing very small values of the modified damage indicators. These are ignored and the values larger than the average value (of the damage indicator) are extracted.

$$\delta\%_j = \begin{cases} MMF\%(2L+V)_j, & MMF\%(2L+V)_j \geq \overline{MMF\%(2L+V)_j} \\ 0, & MMF\%(2L+V)_j < \overline{MMF\%(2L+V)_j} \end{cases}$$

$$Z_j^L = \begin{cases} MMSE_j^L, & MMSE_j^L \geq \overline{MMSE^L} \\ 0, & MMSE_j^L < \overline{MMSE^L} \end{cases}$$

$$Z_j^V = \begin{cases} MMSE_j^V, & MMSE_j^V \geq \overline{MMSE^V} \\ 0, & MMSE_j^V < \overline{MMSE^V} \end{cases}$$

Combining the results of MMF and $MMSE^L$ and result of MMF and $MMSE^V$ as

$$DI_j^L = \begin{cases} \max(\delta\%_j, Z_j^L), & \delta\%_j > 0\ and\ Z_j^L > 0 \\ 0, & \delta\%_j \leq 0\ or/and\ Z_j^L \leq 0 \end{cases}$$

$$\mathrm{DI}_j^V = \begin{cases} \max(\delta\%_j, Z_j^V), & \delta\%_j > 0\ and\ Z_j^V > 0 \\ 0, & \delta\%_j \leq 0\ or/amd\ Z_j^V \leq 0 \end{cases}$$

The improved DI can expressed as

$$DI_j = \begin{cases} DI_j^L, & DI_j^L > 0 \\ DI_j^V, & DI_j^V > 0 \\ \max(DI_j^L, DI_j^V), & DI_j^L > 0\ and\ DI_j^V > 0 \end{cases}$$

4.1 Single damage cases

For the first damage scenario, it was seen in section 2 and 3 that the traditional MSE based (Stubbs) damage index, MSE_j and lateral indicator, $MMSE_j^L$ gave similar results and as the nodal coordinates are shared in this structure, there were large values of the damage index in column elements 17, 18, 26, and 27. Hence damage is not only expected to be "indicated" in the damaged member itself, but also in the members connected to it (Figure 3(b) & 4(b)). However the peak of the vertical indicator, $MMSE_j^V$ clearly indicates the damage in element 22 (Figure 4(a)). This suggests that the contribution to the total modal strain energy from the vertical components is negligibly small in the calculation of MSE_j. In this regard, the improved MCA based DI has shown its capability to clearly locate the damaged beam (22) as shown in Figure 5(a).

The result for the second damage scenario is presented in Figure 5(b). In this case, earlier results show that neither the MSE based damage indicator MSE_j nor the lateral indicator $MMSE_j^L$, can point out the damage accurately (Figure 3(d) & 4(d)), but the vertical indicator, $MMSE_j^V$ (Figure 4(c)), and the MCA based DI (Figure 5(b)) clearly show the damaged element 23. These trends further confirm the results in the first damage scenario.

The results for the third damage case obtained with the original MSE based damage indicator also show a tendency for the damage in the column element to propagate to all beam elements of the model due to the torsional coupling, as seen in Figures 3(f), for the asymmetric models. But the modified indicators and the improved MCA based indicator clearly shows its capability to locate this damage as shown in Figures 4(e) and 4(f) and in Figure 5(c).

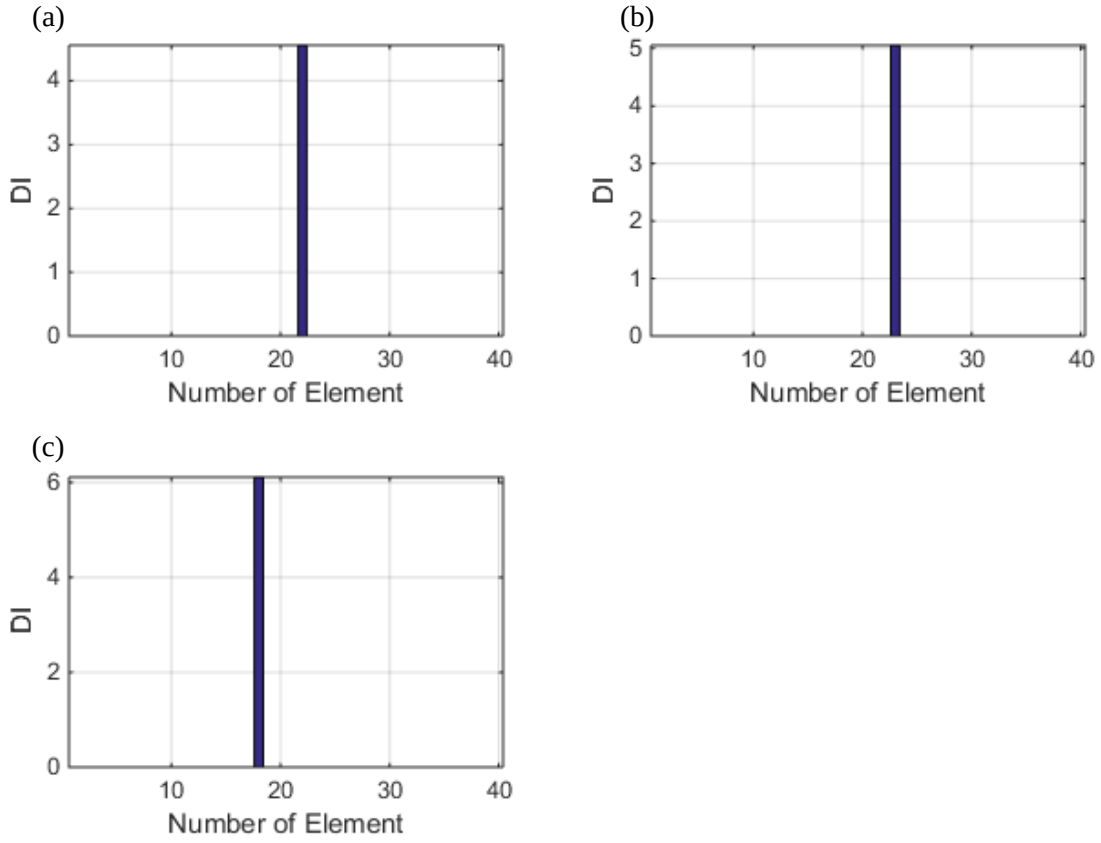

Fig. 5. Results of the MCA based DI (single damage cases) (a) first damage case (b) second damage case and (c) third damage case

4.2 Multiple damage cases

To test the capability of the proposed method in detecting multiple damages, two damage scenarios are considered as shown in Table 2

Results of multiple damage case 4 and case 5 are presented in Figures 6. In case 4, damaged elements are a long span beam and a vertical column element. It is evident that the damaged elements are clearly identified by the two distinct peaks. Damage case 5 pertains to damage in 2 beam and 1 column elements. Again, the results correctly located all damages, though the damage severity is not well defined, probably because only 2 modes were used.

Table 2
Multiple damages cases studied

Case Number	Damaged Element Type	Element Number	Damage Percent (%)
Case 4	long span beam & vertical column	18 & 22	5%
Case 5	long span, short span beam & vertical column	18, 22 & 23	5%

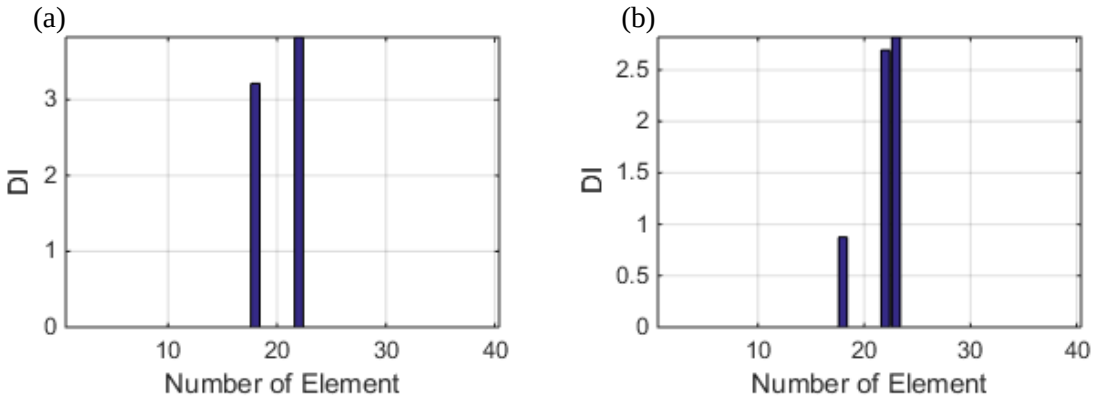

Fig. 6. Results of the MCA based DI (multiple damage cases) (a) forth damage case and (b) fifth damage case

As a brief summary of comparative studies so far, the Stubbs' damage index (or the original MSE based damage index), fails to identify damaged members, in particular for damage in beam elements of the asymmetric model. The proposed modified method shows its capability in locating the damaged member by using only the first two modes. The improved MCA based DI clearly demonstrates its effectiveness in locating damage of asymmetric building structures and eliminates the confusion in using multiple indices.

5 Experimental validation

Before applying the developed technique to full scale models, the modelling techniques will be validated by comparing numerical results with those from experimental testing. Towards this end, a laboratory model of an asymmetric building was designed and constructed as shown in Figure 7. It was designed in such a way that some of the earlier modes were 3 dimensional modes with torsional coupling. The upper floor of the model is made of a right triangular steel plate with dimensions 400mm x 200mm and thickness 3mm supported at each of its 3 corners by a column which is a plain bar of 8mm diameter. The dimensions of lower floor are 800mm in length and 400mm in width, the thickness of the steel plate is 1mm and is supported by 9 plain bars of 8mm in diameter. At the time the test specimen was designed, a corresponding finite

element model of the specimen was developed in ANSYS [30]. It is assumed that there is full connection between the slabs and columns, effectively suppressing all six degrees of freedom.

(a) (b)

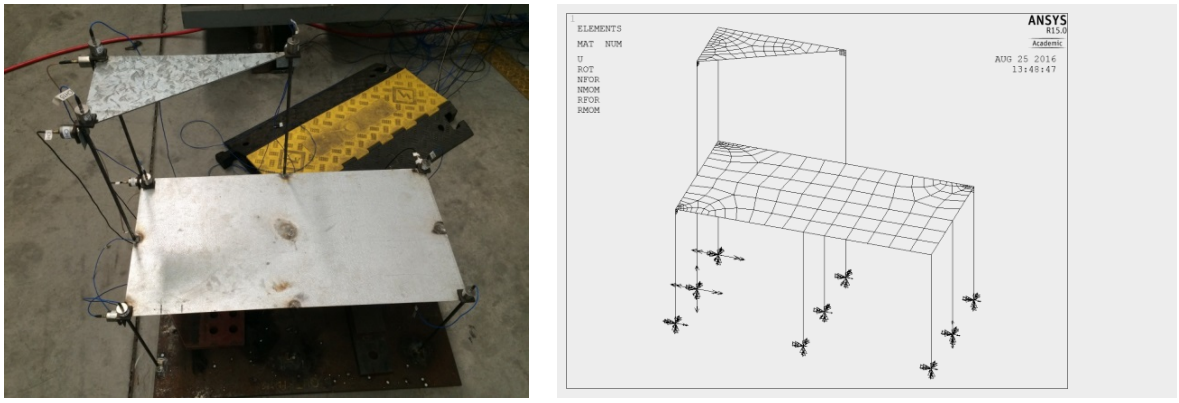

Fig. 7. Laboratory model attached with sensors (a) test specimen and (b) FE model of test specimen

Prior to the free vibration testing, the data acquisition system was established; which included 13 single-axis PCB® 393B05 integrated circuit piezoelectric, positioned to measure vertical and lateral accelerations. All sensors were self-calibrated; this means after a small period the sensors are able to automatically pickup correct acceleration without further calibrations. The sensors are able to measure a signal in the frequency range between 0.7 Hz to 450 Hz (±5%) with sensitivity of 10V/m/s2 (±10%). They are attached to the test specimen using the N42 Rare Earth Magnets. The experimental vibration system consists of three main components; (i) impact hammer (ii) accelerometers and (iii) data acquisition system. The impact hammer is used to provide a source of excitation to the test specimen. The accelerometers are used to convert the mechanical motion of the structure into an electrical signal. The Software "SignalExpress" is used to execute signal processing and the Operational Modal Analysis (OMA) software "ARTeMIS is then used to process the modal analysis.

The free vibration test was conducted in undamaged state of the structure which is considered as baseline structure. The 2nd and 3rd dynamic tests were conducted at the damaged states with damage extents of 10% and 40% reductions in stiffness (obtained by reducing the diameter across a length of 100 mm since stiffness is proportional to cross section of the element) in the cross-section of the 9th column element (to enhance the validation of the FE model) as shown in Figure 8. The free vibration measurement is an output data-only dynamic testing where the wind and human activities are used as natural ambient excitations. Since the specimen was placed in the laboratory and not subjected to any ambient loading, artificial excitation was adopted. In an effort to excite the structure, random tapping was provided through an impact hammer made of foam (to reduce the negative impact). All the acceleration data was captured in the time domain by DAQ system while conducting the experiment and was then transferred to the ARTeMIS modal analysis software to obtain modal parameters.

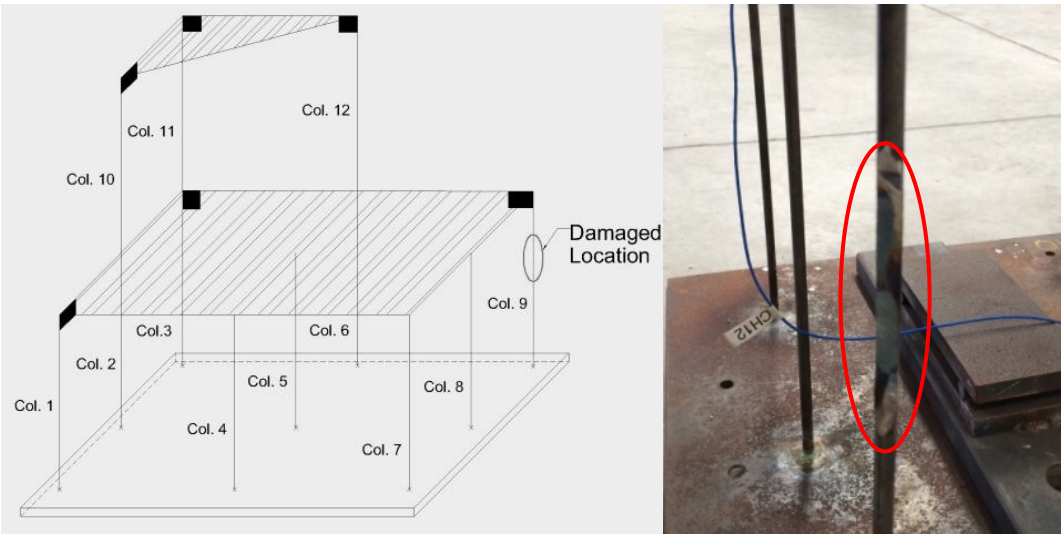

Fig. 8. Flaw at steel bar of the model

The natural frequencies and mode shapes were determined by SSI-DATA (UPC) in ARTeMIS modal analysis software. A comparison between numerical and experimental dynamic characteristics was conducted and presented in Table 3. Model updating was done to tune in the structural parameters of the FE model such that natural frequencies obtained in the experiment and FE model closely match. With the change of structural parameters such as connectivity of structural elements, support conditions and Young's Modulus, the initial FE model was updated to match the measured natural frequencies as close as possible. The comparison of natural frequencies of the test model and those obtained from FE analysis is done by calculating the relative error $f_{error} = \frac{(f_{exp} - f_{fem})}{f_{exp}} \times 100$, where f_{exp} is natural frequency obtained in the experiment and f_{fem} is the corresponding natural frequency obtained in the FE analysis.

Table 3
Correlation between experimental and FE model

Mode	Undamaged			10% damaged			40% damaged		
	Natural Frequency (Hz)		f_{error} (%)	*Natural Frequency (Hz)*		f_{error} (%)	*Natural Frequency (Hz)*		f_{error} (%)
	f_{exp}	f_{fem}		f_{exp}	f_{fem}		f_{exp}	f_{fem}	
1	6.418	6.4087	0.14	6.406	6.3989	0.11	6.37	6.3602	0.15
2	6.869	6.8127	0.82	6.881	6.8065	1.08	6.848	6.7825	0.96
3	12.426	12.783	-2.87	12.346	12.748	-3.26	12.125	12.604	-3.95
4	17.535	17.972	-2.49	17.491	17.959	-2.68	17.416	17.893	-2.74
5	19.645	19.865	-1.12	19.614	19.858	-1.24	19.601	19.812	-1.08

The difference between the measured and computed natural frequencies of the test specimen is smaller than 4%, which demonstrates a very good correlation of results. It is hence evident from Table 3 that the natural frequencies obtained from the experiment and FE analysis compare reasonably well. Mode shapes were compared by calculating MAC values, which vary from 0 to 1, with 0 for no correlation and 1 for full correlation. It can be seen from Table 4 that the 2 sets of mode shapes compare reasonably well. It is hence concluded that the measured and

computed natural frequencies and mode shapes are in good agreement and provide confidence in the modelling techniques used in this study.

Table 4
MAC values comparing experimental and analytical data

Undamaged model		Analytical data				
		Mode 1	**Mode 2**	**Mode 3**	**Mode 4**	**Mode 5**
Experimental data	**Mode 1**	0.9820	0.9559	0.5441	0.3537	0.5006
	Mode 2	0.9346	0.9974	0.7180	0.5214	0.5780
	Mode 3	0.3443	0.5377	0.8931	0.8456	0.4004
	Mode 4	0.4474	0.6152	0.7967	0.9325	0.3261
	Mode 5	0.4297	0.5052	0.3620	0.3260	0.9902

To confirm the feasibility of proposed method in detecting damage, the measured natural frequencies and associated mode shapes obtained from the free vibration testing of both the intact and damaged test models are used to plot the MCA based DIs for the two damage cases as shown in Figure 9. It is evident that there is a distinct peak in each of these figures corresponding to the position of the damaged element. These results conform well to the damage scenario. Even though only three modes obtained from the experimental testing were used to evaluate the damage detection parameters, they are able to predict the damage location quite well. This establishes that the chosen MCA based DI is competent in locating damage in the test structure and provides further confidence in damage detection in asymmetric building structures using the proposed procedure.

The validation of the modelling techniques by comparison of the experimental and computed results for frequencies, mode shapes and MAC values for both the healthy and the damaged building models and the establishment of the feasibility of the chosen damage detection indices (as described earlier) provide adequate confidence in the procedure used in this paper for damage detection in asymmetric buildings and ensure its application to realistic full scale building models.

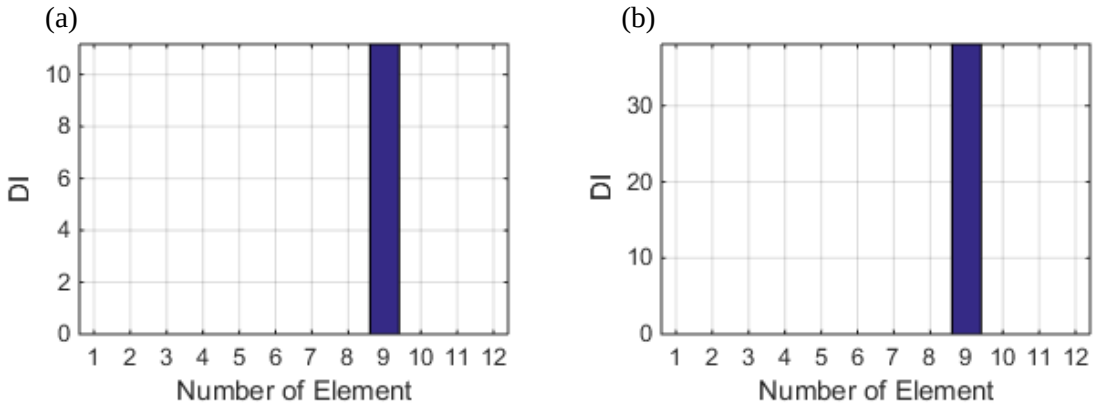

Fig. 9. Results of experimental damage detection (a) first damage case and (b) second damage case

6 Conclusion

A procedure to detect and locate damage in an asymmetric building structure has been developed and presented in this paper. It uses a multi-criteria approach (MCA) to complement and supplement the results of MMSE and MMF methods to obtain reliable outcomes. The

contribution of this research can be captured by the process that was developed in three stages. First, comparative investigation of damage detection in three-dimensional symmetric and asymmetric buildings was conducted, before the dynamic behaviour of two proposed models was briefly reviewed. Next, the comparison of damage detection results between the symmetric and asymmetric model was made. Based on these findings, a modified approach was developed from Stubbs' modal strain energy damage index by decomposing it into two separate damage indices that use either the lateral or vertical components of the mode shapes. The last stage was to incorporate the proposed MMSE with MMF in the damage detection procedure so that the results can be compared to provide the best chance of obtaining reliable results in damage detection.

The procedure was first illustrated through numerical studies conducted on three dimensional five-story symmetric and asymmetric frame structures with the same layout. Three single damage scenarios were considered in the numerical simulations with damage in a longer-span beam, a short-span beam and a single column. The other two damage scenarios considered multiple damage locations with either damage in both a beam and a column or two beams and a column. Vibration parameters obtained from finite element analysis of the intact and damaged building models were then applied into the proposed algorithms for detecting and locating the damage in these buildings. The results showed that the Stubbs' damage index algorithm fails to identify damaged members particularly for beam elements. The proposed MMSE method using the vertical or the horizontal damage index was shown to be capable of locating the damage in either a horizontal beam or a vertical column reasonably well. However, as there will be no prior knowledge of the damage location in real life, the MMF method was incorporated as it can be a good indicator to confirm whether the damage is in a beam or a column element.

As there are still some drawback in each method, the improved MCA method incorporating the three damage indices was developed and applied to the three damage scenarios. The application result has clearly shown capability of the MCA method for accurate damage detection. The modelling techniques and the proposed MCA method are then validated through experimental testing of a laboratory scale asymmetric building model. It can be concluded that (1) different from the symmetric building model, there is torsional coupling in both the first two modes of the asymmetric model, (2) due to torsional coupling in the structure, the damage in one member of the structure has a tendency to influence the other elements, (3) the modified method incorporating mode shape component specific damage indicators are reasonably effective in detecting damage in both the horizontal and vertical members of the asymmetric building model, and (4) the improved MCA method demonstrates a very effective way in locating damage of asymmetric building structures and eliminates the confusion in simultaneously using multiple indices. The procedure developed in this research can be extended to detect and locate damage in different types of asymmetric buildings including normal high-rise buildings, multi-propose towers, etc.

Acknowledgments

This paper forms a part of a continuing study of structural health monitoring of structures conducted at the Queensland University of Technology, Australia. Yi Wang gratefully acknowledges the support of this research provided by the Queensland University of Technology Postgraduate Research Award and International Postgraduate Research Scholarship.

References

[1] S.J. Ansari, S. Bhole, Comparative Study of Symmetric & Asymmetric L-Shaped & T-Shaped Multi-Storey Frame Building Subjected to Gravity & Seismic Loads with Varying Stiffness, International Journal of Science Technology & Engineering, 2 (2016) 734-742.
[2] L. Dowling, G. Rummey, Guidelines for Bridge Management: Structure Information, (2004).

[3] T.H. Chan, K. Wong, Z. Li, Y.-Q. Ni, Structural health monitoring for long span bridges: Hong Kong experience and continuing onto Australia, Structural Health Monitoring in Australia, (2011) 1-32.
[4] D. Balageas, C.-P. Fritzen, A. Güemes, Structural health monitoring, Wiley Online Library, 2006.
[5] H.W. Shih, D. Thambiratnam, T.H. Chan, Damage detection in truss bridges using vibration based multi-criteria approach, Structural Engineering and Mechanics, 39 (2011) 187-206.
[6] P. Rizos, N. Aspragathos, A. Dimarogonas, Identification of crack location and magnitude in a cantilever beam from the vibration modes, Journal of sound and vibration, 138 (1990) 381-388.
[7] J.-C. Hong, Y. Kim, H. Lee, Y. Lee, Damage detection using the Lipschitz exponent estimated by the wavelet transform: applications to vibration modes of a beam, International journal of solids and structures, 39 (2002) 1803-1816.
[8] H.W. Shih, D.P. Thambiratnam, T.H. Chan, Vibration based structural damage detection in flexural members using multi-criteria approach, Journal of sound and vibration, 323 (2009) 645-661.
[9] P. Cornwell, S.W. Doebling, C.R. Farrar, Application of the strain energy damage detection method to plate-like structures, Journal of Sound and Vibration, 224 (1999) 359-374.
[10] A. Messina, T. Contursi, E.J. Williams, A Multiple-Damage Location Assurance Criterion Based on Natural Frequency Changes, Journal of Vibration and Control, 4 (1998) 619-633.
[11] Z. Shi, S. Law, L. Zhang, Damage localization by directly using incomplete mode shapes, Journal of Engineering Mechanics, 126 (2000) 656-660.
[12] S. Law, Z. Shi, L. Zhang, Structural damage detection from incomplete and noisy modal test data, Journal of Engineering Mechanics, 124 (1998) 1280-1288.
[13] J.S.-L. Hu, S. Wang, H. Li, Cross-modal strain energy method for estimating damage severity, Journal of engineering mechanics, 132 (2006) 429-437.
[14] K. Morita, M. Teshigawara, T. Hamamoto, Detection and estimation of damage to steel frames through shaking table tests, Structural Control and Health Monitoring, 12 (2005) 357-380.
[15] S. Wang, J. Zhang, J. Liu, F. Liu, Comparative study of modal strain energy based damage localization methods for three-dimensional structure, in: The Twentieth International Offshore and Polar Engineering Conference, International Society of Offshore and Polar Engineers, 2010.
[16] F. Liu, H. Li, W. Li, B. Wang, Experimental study of improved modal strain energy method for damage localisation in jacket-type offshore wind turbines, Renewable Energy, 72 (2014) 174-181.
[17] H. Li, H. Yang, S.-L.J. Hu, Modal strain energy decomposition method for damage localization in 3D frame structures, Journal of engineering mechanics, 132 (2006) 941-951.
[18] F.L. Wang, T.H.T. Chan, D. Thambiratnam, A. Tan, C. Cowled, Correlation-based damage detection for complicated truss bridges using multi-layer genetic algorithm, Advances in Structural Engineering, 15 (2012) 693-706.
[19] H. Shih, D. Thambiratnam, T.H.T. Chan, Damage detection in slab-on-girder bridges using vibration characteristics, Structural Control and Health Monitoring, 20 (2013) 1271-1290.
[20] W. Fan, P. Qiao, Vibration-based damage identification methods: a review and comparative study, Structural Health Monitoring, 10 (2011) 83-111.
[21] C.R. Farrar, H.Y. Sohn, Condition/damage monitoring methodologies, in, Los Alamos National Laboratory, 2001.
[22] E. Manoach, I. Trendafilova, Large amplitude vibrations and damage detection of rectangular plates, Journal of sound and vibration, 315 (2008) 591-606.
[23] C. Cempel, H. Natke, A. Ziolkowski, Application of transformed normal modes for damage location in structures, in: Structural integrity assessment, 1992, pp. 246-255.
[24] A. Pandey, M. Biswas, Damage detection in structures using changes in flexibility, Journal of sound and vibration, 169 (1994) 3-17.
[25] N. Stubbs, J.-T. Kim, Damage localization in structures without baseline modal parameters, Aiaa Journal, 34 (1996) 1644-1649.

[26] N. Stubbs, J.-T. Kim, C. Farrar, Field verification of a nondestructive damage localization and severity estimation algorithm, in: Proceedings-SPIE the international society for optical engineering, SPIE INTERNATIONAL SOCIETY FOR OPTICAL, 1995, pp. 210-210.
[27] F. Au, Y. Cheng, L. Tham, Z. Bai, Structural damage detection based on a micro-genetic algorithm using incomplete and noisy modal test data, Journal of Sound and Vibration, 259 (2003) 1081-1094.
[28] Z. Shi, S. Law, L. Zhang, Structural damage localization from modal strain energy change, Journal of Sound and Vibration, 218 (1998) 825-844.
[29] Z. Shi, S. Law, L.M. Zhang, Structural damage detection from modal strain energy change, Journal of engineering mechanics, 126 (2000) 1216-1223.
[30] ANSYS Inc., ANSYS Mechanical APDL Academic Research, in, Canonsburg PA, 2011.
[31] A. Berman, W.G. Flannelly, Theory of incomplete models of dynamic structures, AIAA journal, 9 (1971) 1481-1487.
[32] W.R. Wickramasinghe, D.P. Thambiratnam, T.H.T. Chan, T. Nguyen, Vibration characteristics and damage detection in a suspension bridge, Journal of Sound and Vibration, 375 (2016) 254-274.